

# Longitudinal Structure/Function Analysis in Reticular Pseudodrusen

Florian Alten, Peter Heiduschka, Christoph R. Clemens, and Nicole Eter

Department of Ophthalmology, University of Muenster Medical Center, Muenster, Germany

Correspondence: Florian Alten, Department of Ophthalmology, University of Muenster Medical Center, Domagkstrasse 15, 48149 Muenster, Germany; [florian.alten@ukmuenster.de](mailto:florian.alten@ukmuenster.de).

Submitted: December 19, 2013

Accepted: August 11, 2014

Citation: Alten F, Heiduschka P, Clemens CR, Eter N. Longitudinal structure/function analysis in reticular pseudodrusen. *Invest Ophthalmol Vis Sci*. 2014;55:6073–6081. DOI: 10.1167/iovs.13-13804

**PURPOSE.** To describe longitudinal structure/function correlations in eyes with progressive reticular pseudodrusen (RPD).

**METHODS.** Thirteen eyes of 12 patients with exclusively RPD in the posterior pole were included ( $75.1 \pm 5.7$  years). All patients underwent spectral-domain optical coherence tomography (SD-OCT), confocal scanning laser ophthalmoscopy (cSLO), and multifocal electroretinography (mfERG) at baseline and 12-month follow-up. Size of retinal area affected by RPD, number and stages of RPD lesions, and choroidal thickness (CT) were quantified at baseline and at follow-up visit. Amplitudes obtained by mfERG in RPD eyes at baseline and follow-up were analyzed and correlated to morphologic changes. Eyes were compared to those of age-matched healthy controls.

**RESULTS.** The total number of RPD lesions increased from 540 at baseline to 667 at 12-month follow-up. Mean CT was  $198.5 \pm 69.3 \mu\text{m}$  at baseline (control group  $263.5 \pm 42.6 \mu\text{m}$ ;  $P = 0.005$ ) and  $189.2 \pm 65.3 \mu\text{m}$  at follow-up ( $P < 0.001$ ) (control group  $265 \pm 47.8 \mu\text{m}$ ;  $P = 0.74$ ). A mean growth of RPD-affected area of  $3.3 \text{ mm}^2$  was measured. Multifocal ERG amplitudes decreased in both the study and control groups to a similar extent. Amplitudes differed significantly at the follow-up time point when compared between RPD-affected and nonaffected areas within the same eye. No correlations between changes of morphologic parameters and mfERG amplitude changes were found.

**CONCLUSIONS.** Multifocal ERG allows for detecting a decline of function over time in eyes with progressive RPD. Yet functional decline could not be correlated to changes in individual morphologic parameters.

**Keywords:** age-related macular degeneration, reticular drusen, reticular pseudodrusen, subretinal drusenoid deposits, multifocal electroretinography, confocal scanning laser ophthalmoscopy, spectral-domain optical coherence tomography

Reticular pseudodrusen (RPD) have been recognized as an additional phenotypic characteristic frequently observed in patients with age-related macular degeneration (AMD). Several studies have proven that the prevalence of RPD is associated with AMD as well as a high risk of disease progression to late forms of AMD.<sup>1–9</sup>

Multifocal electroretinography (mfERG) allows a localized assessment of retinal function providing a topographic map of the central retinal electrophysiological activity.<sup>10,11</sup> Multifocal ERG proved to be a useful, reliable, and sensitive biomarker in the quantitative assessment of localized retinal function in eyes with nonexudative forms of AMD.<sup>12–14</sup> Contrary to other phenotypic characteristics of AMD, we previously reported that mfERG measurements do not show definite interference of electrophysiological activity in retinal areas affected exclusively with RPD, representing the first structure/function analysis of RPD.<sup>15</sup>

Interestingly, recent reports proved an anatomic progression of RPD lesions over time. A growth in terms of lesion height was observed using spectral-domain optical coherence tomography (SD-OCT), and an increase in affected retinal area size was documented in the course of the disease by means of confocal scanning laser ophthalmoscopy (cSLO), suggesting that RPD are dynamic structures and subject to morphologic

changes over time.<sup>16,17</sup> Earlier studies revealed a reduced choroidal thickness (CT) and choroidal volumes in patients with RPD.<sup>18,19</sup> Additionally, Spaide<sup>20</sup> reported data of a 3-year follow-up study in AMD patients demonstrating a choroidal thinning in the retinal area affected by RPD, yet added a third specific morphologic parameter that dynamically evolves over time, characterizing a progression of the RPD phenotype.

These findings raise the question whether longitudinal structural changes associated with RPD in AMD patients have an impact on retinal function. Thus, the aim of our study was to find correlations between morphologic parameters of RPD progression and alterations in retinal function over time by means of mfERG and combined simultaneous cSLO and SD-OCT.

## METHODS

### Demographics

Participants were recruited from the medical retina clinic of the Department of Ophthalmology at University of Muenster Medical Center. Only patients with distinct RPD in combined simultaneous cSLO and SD-OCT imaging of the posterior pole in one or both eyes were considered. Eyes were not eligible if any

signs of conventional drusen, choroidal neovascularization (CNV), geographic atrophy (GA), or pigment epithelium detachment due to AMD were observed in funduscopy, SD-OCT, cSLO, or fluorescence angiography. Intravitreal anti-VEGF therapy and vitreoretinal surgery in the medical history as well as other vascular or inflammatory retinal pathologies also led to exclusion. Eyes with dense lens opacities, corneal opacities, refractive surgery, or a history of intraocular inflammation were not considered either. Further exclusion criteria were refractive error > 2 diopters due to the described relation of myopia and choroidal thinning.<sup>21,22</sup>

We included 13 eyes of 12 patients with RPD in the posterior pole (5 females and 7 males, age  $75.1 \pm 5.7$  years) for the baseline visit between July 2011 and October 2012. In the study group, 6 fellow eyes had a CNV, 2 showed GA, 3 had significant soft drusen, and 1 patient had exclusively RPD. Apart from the 13 study eyes, six previously screened RPD eyes of six patients could not be included in the study group due to GA, CNV, or significant soft drusen development before inclusion or during the follow-up period.

Best corrected visual acuity (BCVA) better than 0.5 of the study eye was required to ensure stable fixation during mfERG measurement. A total of 13 eyes of 10 healthy control subjects (5 females and 5 males, age  $71.1 \pm 4.8$  years) without RPD or any other retinal pathology served as a control group. All control subjects also underwent the same examination protocol as the RPD group. Healthy control eyes were age matched to RPD eyes. Informed consent was obtained from all participants before testing. The research followed the tenets of the Declaration of Helsinki. Participants in the study group and in the healthy control group underwent the imaging protocol as well as mfERG measurements at baseline and after 12 months as previously described in detail.<sup>15</sup> Characteristics of RPD lesions in different imaging modalities have been reported in detail elsewhere.<sup>15</sup>

Three previously described parameters characterizing longitudinal morphologic progression of the RPD phenotype are evaluated and correlated to functional mfERG measurements: progression of RPD stages, CT superior to the fovea, and RPD-affected retinal area size.<sup>16,17,19</sup>

### Progression of RPD Stages

Spectral-domain OCT images were obtained by using  $25^\circ \times 30^\circ$  macular volume scans consisting of 61 equally spaced horizontal averaged B-scans at baseline and follow-up. Scans were saved for analysis after 50 frames were averaged using the automatic averaging and eye-tracking features (Spectralis; Heidelberg Engineering, Heidelberg, Germany). Additionally to cSLO images, SD-OCT scans were used to prove the presence of RPD and the absence of other retinal pathologies in the study group and to prove the integrity of all retinal layers in the healthy controls. The eye tracker function allows reliable detection of small morphologic changes over time. Despite the eye tracker follow-up protocol of the Spectralis device, exact point-to-point correlation between baseline and follow-up scan position cannot be assumed without critical review, particularly when evaluating small alterations like single RPD lesions. Attributing single RPD lesions to defined classification stages requires OCT scans exactly depicting the lesion's center in order to judge the true lesion's height. Exact positioning of follow-up scans is crucial, as lesions may be easily misclassified if follow-up scans vary only slightly in their position compared to baseline examination and thus the lesion's height is not depicted correctly. For instance, an RPD lesion stage 3 at baseline may be misinterpreted as a lesion stage 2 at follow-up examination if the initial OCT scan runs through the exact center of the

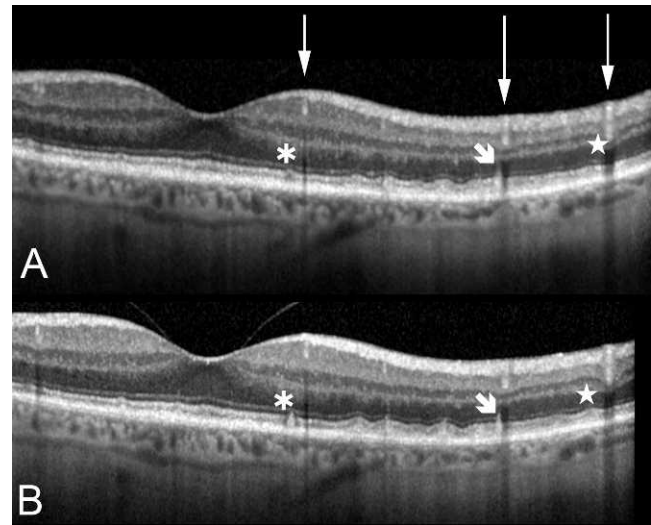


**FIGURE 1.** (A, B) Spectral-domain optical coherence tomography (SD-OCT) in a patient showing change of lesion height of reticular pseudodrusen (RPD) at baseline (A) and at 12-month follow-up visit (B). Arrows point to retinal vessel crossings proving a good alignment between baseline and follow-up scan. Asterisks mark a lesion developing from stage 2 to 3. Arrowheads show a RPD lesion that appears not to have changed during study period. Stars mark a lesion that progressed from stage 1 to 2.

RPD lesion while the follow-up scan cuts the same lesion eccentrically. To achieve a higher amount of accuracy in RPD stage grading over time, five high-quality tracked scans per study eye were selected and included in the analysis; these showed the exact same scan positioning with regard to invariant anatomic reference points, particularly blood vessels. Thus, only a part of all the RPD lesions present was evaluated, yet thereby a higher degree of reliability was achieved. For each pair of baseline and follow-up scans included in the analysis, all RPD lesions were evaluated and graded by two expert retinal physicians (CRC, FA) according to the previously reported classification (Fig. 1).<sup>16,23</sup> Disagreement between readers regarding stage classification was resolved by open adjudication.

### Choroidal Thickness Superior to the Fovea

According to SD-OCT scans as described above, enhanced depth imaging (EDI) OCT volume scans were obtained at baseline and at the follow-up visit. Enhanced depth imaging scans were viewed and CT was measured using the integrated software package (Heidelberg Eye Explorer software, version 1.7.0.0; Heidelberg Engineering). Choroidal thickness measurements were performed from the outer portion of the hyperreflective line corresponding to the retinal pigment epithelium to the inner surface of the sclera. As previously described by Spaide<sup>20</sup> in a longitudinal RPD study, measurements were performed by two retinal physicians (FA, CRC) at 2 mm superior from the foveal center at baseline and at the follow-up visit (Fig. 2).

### RPD-Affected Retinal Area Size

Confocal SLO retinal imaging (Spectralis) included acquisition of near-infrared reflectance (IR; 820 nm) and fundus autofluorescence (FAF; excitation 488 nm, emission 500–700 nm) at baseline and follow-up visit. The field of view was set at  $30^\circ \times 30^\circ$  and centered on the macula. For the measurement of retinal area size affected by RPD lesions, a

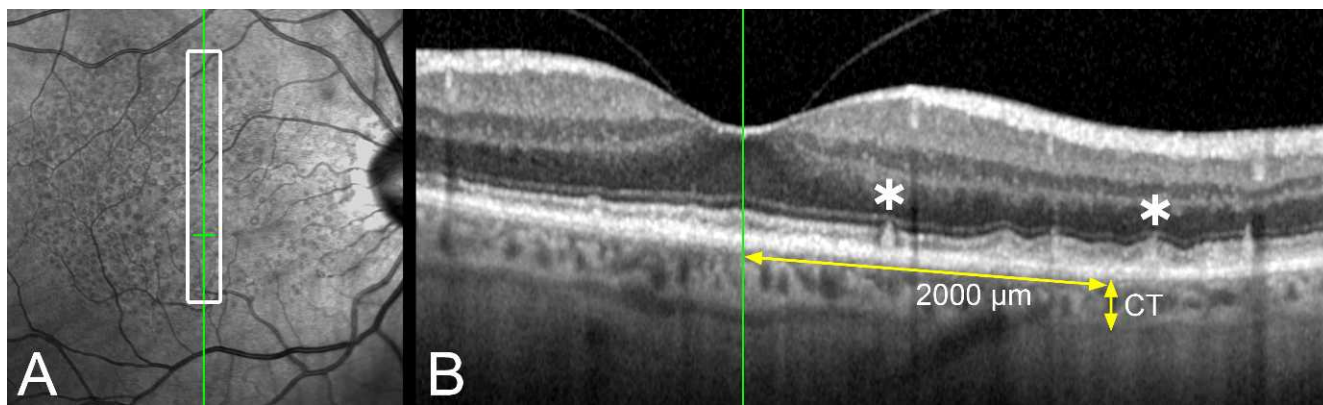


**FIGURE 2.** (A, B) Combined simultaneous confocal scanning laser ophthalmoscopy (cSLO) and spectral-domain optical coherence tomography (SD-OCT) in a patient showing reticular pseudodrusen (RPD). (A) cSLO infrared image with *green line* indicating the vertical scan through the center of the fovea. The *green cross* indicates the central fovea and the corresponding localization of the *green line* in (B). The *rectangle* indicates the scan section shown aside. (B) SD-OCT scan showing manual choroidal thickness (CT) measurement 2 mm superior to the central fovea, which was performed by two independent readers. *Asterisks* mark exemplary RPD lesions.

convex hull was employed that was introduced by Schmitz-Valckenberg and colleagues<sup>17,24</sup> and proved to be a practical and reproducible method for analyzing ill-defined lesion boundaries in retinal imaging. Obviously, the measurement is rather an estimation for the actual affected area, for borders of RPD-affected areas are composed of subtle irregular lesions that often do not allow an exact border delineation. If the RPD boundaries exceeded any part of the edge of the cSLO image, the convex hull was drawn at the border of the image. In this case, the convex hull area represents the minimum retinal area affected by RPD. Thus, it was defined as the minimum convex polygon encompassing the entire RPD area.<sup>17</sup> To determine the RPD area, the convex hull was manually outlined using the measuring tool of the integrated software at both baseline and the 12-month visit by two independent readers (CRC, FA) who were blinded to the study visit (Fig. 3). Pixel area values are automatically converted to square millimeters. Mean values of RPD area measurements of both readers at baseline were subtracted from mean area values of both readers at the follow-up visit to calculate RPD area progression over time.

**Multifocal ERG**

All baseline and follow-up recordings were performed with a RetiPort System (Roland Consult, Brandenburg an der Havel, Germany) according to the latest International Society for Clinical Electrophysiology of Vision guidelines.<sup>25</sup> Good fixation during mfERG measurements was warranted by the technician and by a sufficient BCVA of the participants. To ensure good intersession reproducibility, all measurements were performed by the same experienced operator.

Evaluation of mfERG measurements has been previously described.<sup>15</sup> Briefly, two methods were chosen. Firstly, responses of single retinal fields with and without RPD were compared. In each study eye, 10 of the 103 mfERG fields with RPD and the opposite fields without RPD were identified. As a result, 10 matched pairs were obtained (method 1). Fields were excluded that initially did not show RPD at baseline but showed RPD lesions at follow-up examination due to RPD progression. Secondly, macular quadrants were compared. The macula was divided into four retinal fields of equal size. Depending on the individual distribution of RPD, the quadrant most affected by RPD and the opposite quadrant least affected by RPD were identified,

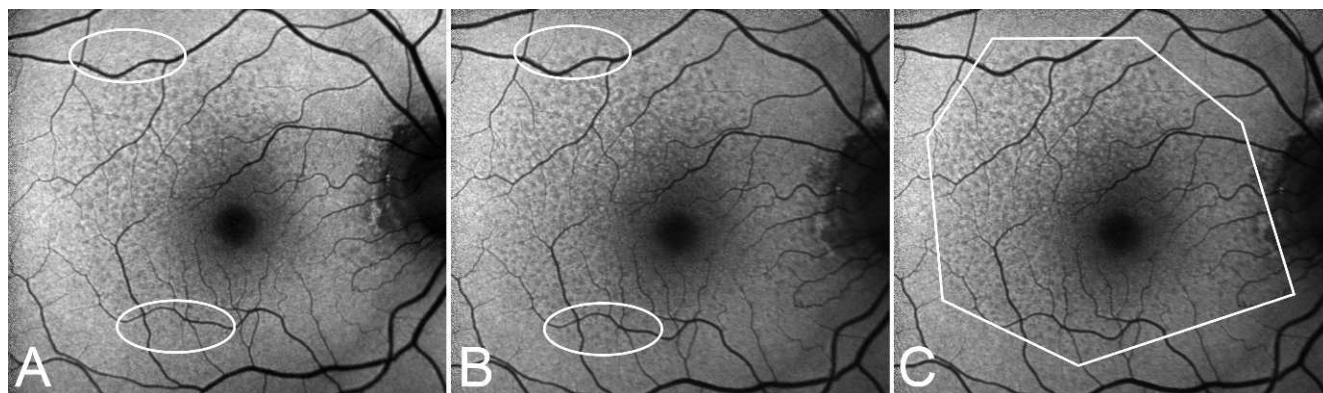


**FIGURE 3.** (A–C) Confocal scanning laser ophthalmoscopy (cSLO) fundus autofluorescence (FAF) imaging in a patient showing progression of reticular pseudodrusen (RPD)-affected retinal area at baseline (A) and at 12-month follow-up visit (B). RPD show their typical appearance of a regular network of lesions exhibiting a decreased FAF signal, sometimes with an increased FAF signal in the lesion's center. *Ovals* indicate exemplary regions of growth in RPD-affected area suggesting a centrifugal spread. The lesions' density appears lower at the border of affected areas. (C) FAF image of the same patient illustrates application of the convex hull used for area quantification defined as the minimum polygon encompassing the RPD-affected retinal field.

**TABLE.** Demographic and Morphologic Data of Study Patients and Healthy Control Patients

	Baseline	Follow-Up	P Value
Patients, <i>n</i> = 12			
Age, mean	75.1	-	-
Female, <i>n</i> (%)	5 (41.7)	-	-
Eyes, <i>n</i> = 13			
BCVA, mean	0.92	0.80	0.125
RPD, <i>n</i> = 13			
Stage, <i>n</i>			
1	89	87	>0.9999
2	336	403	0.027
3	113	178	0.003
4	2	9	0.062
RPD-affected area, mm <sup>2</sup>			
Mean area	23.0	26.3	0.0002
Mean difference R1-R2	1.00	0.81	0.358
Choroidal thickness, μm			
Study group	198.5	189.2	0.005
Control group	263.5	264.9	0.986

R1, reader 1; R2, reader 2.

and matched pairs of mfERG measurement fields lying exactly on the opposite sites within these two quadrants were compared (method 2).<sup>15</sup> Both methods were applied to the control group. Study eyes were age matched to control eyes, and the same retinal fields and quadrants as in the RPD eyes were used in the control eyes for comparison.

Besides the comparison between baseline and follow-up measurements, data were also analyzed for correlations between functional mfERG measurements and the three described morphologic parameters.

**Statistical Methods**

Data were exported from the Roland Consult RetiPort software to Excel files and imported into the Microsoft (Redmond, WA, USA) Excel program for further analysis. Statistical significance of the differences between data obtained in areas with or without RPD and the differences between the corresponding retinal fields in the control group was calculated by Mann-Whitney test and the Wilcoxon signed-rank test. Morphological data were also compared using the Wilcoxon signed-rank test. Statistical significance was set at *P* < 0.01.<sup>26</sup>

**RESULTS**

**Demographics**

Best corrected visual acuity was 0.92 ± 0.09 at baseline and 0.85 ± 0.14 at follow-up visit (*P* = 0.125). In the control group, BCVA changed from 0.91 ± 0.12 to 0.86 ± 0.16 (*P* = 0.25). There was no significant difference in BCVA values between the patient and control groups (*P* = 1.0 at baseline and *P* = 0.838 at follow-up). Time interval between baseline and the follow-up visit was 12.5 months for the study group and 12.9 months for the control group. Mean refractive error was 0.40 ± 1.36 diopters for eyes affected with RPD and 0.35 ± 1.24 diopters for healthy control eyes (*P* = 0.95). In three study eyes, OCT revealed development of soft drusen over the follow-up period. However, the number of soft drusen did not exceed three single lesions. None of the study eyes showed

GA or CNV at the follow-up visit. Healthy controls did not develop any kind of retinal pathology in the course of the study period.

**Progression of RPD Stages**

Overall, five pairs of high-quality SD-OCT B-scans (both baseline and follow-up examinations) of each study eye were included in the analysis. A total of 540 RPD lesions (a mean of 8.3 RPD per scan and 41.5 RPD per patient) were graded by two experienced graders at the baseline examination. Eighty-nine RPD lesions (16.5%) were graded as stage 1; 336 (62.2%) were graded as stage 2; 113 (20.9%) as stage 3; and 2 (0.4%) as stage 4. At 12-month follow-up, the total number of detectable RPD lesions was 667 (87 [12.9%], 403 [59.5%], 178 [26.3%], 9 [1.3%]) (Table, Fig. 4). The increase of RPD number was highly significant (*P* < 0.001).

**Choroidal Thickness Superior to the Fovea**

The mean CT was significantly reduced in the study group with RPD compared to the control group at baseline (198.5 ± 69.3 μm; control group 263.5 ± 42.6 μm; *P* = 0.005). Mean CT further decreased in the study group over time (189.2 ± 65.3 μm; *P* < 0.001) while CT was stable in the control group (265 ± 47.8 μm; *P* = 0.74) (Table, Fig. 4). The mean baseline difference for interobserver agreement was 8.54 ± 4.63 μm (follow-up 8.15 ± 3.83 μm) in the study group and 9.54 ± 6.28 μm (follow-up 9.46 ± 3.64 μm) in the control group.

**RPD-Affected Retinal Area Size**

At baseline, the mean area size of RPD-affected retina was 23.0 ± 12.9 mm<sup>2</sup>. The mean baseline difference for interobserver agreement was 1.0 ± 0.7 mm<sup>2</sup> (follow-up 0.8 ± 0.6 mm<sup>2</sup>). At follow-up visit, the average RPD-affected area size was 26.3 ± 14.4 mm<sup>2</sup> (*P* < 0.001), resulting in a mean RPD area growth rate of 3.3 mm<sup>2</sup>/year (Table, Fig. 4). In three eyes, RPD involvement exceeded the image frames at both baseline and at follow-up examination particularly superior to the fovea.

**Multifocal ERG**

Multifocal ERG measurements could be performed in all patients and controls successfully at baseline and follow-up time points.

We observed decreased mfERG amplitudes in both the study group and the healthy control group during the 1-year follow-up. Mean amplitudes measured in the areas affected by RPD were 20.4 to 48.9 nV/deg<sup>2</sup> (control group 13.4–37.2 nV/deg<sup>2</sup>) at baseline and decreased to 16.0 to 32.8 nV/deg<sup>2</sup> (14.5–31.5 nV/deg<sup>2</sup>). In the study group, mean mfERG amplitudes measured in the area affected by RPD decreased down to 77.8 ± 14.9% (method 1) or 82.2 ± 21.5% (method 2), and mean mfERG amplitudes obtained in equivalent areas in healthy controls decreased down to 88.1 ± 22.5% (method 1) or 89.7 ± 19.7% (method 2) (Fig. 5). There was no significant difference in changes of mfERG amplitudes between the two groups, regardless of whether method 1 or method 2 was applied and regardless of whether comparison was performed between unpaired data or age-matched pairs of patients and controls were compared (*P* values between 0.31 and 0.73). Comparing the group of three patients who developed small single soft drusen to the other study eyes, no significant difference was observed regarding mfERG amplitudes and CT.

Similarly, no significant differences were found between changes in mfERG amplitudes obtained in patients and controls when nonaffected areas were evaluated (not shown). In

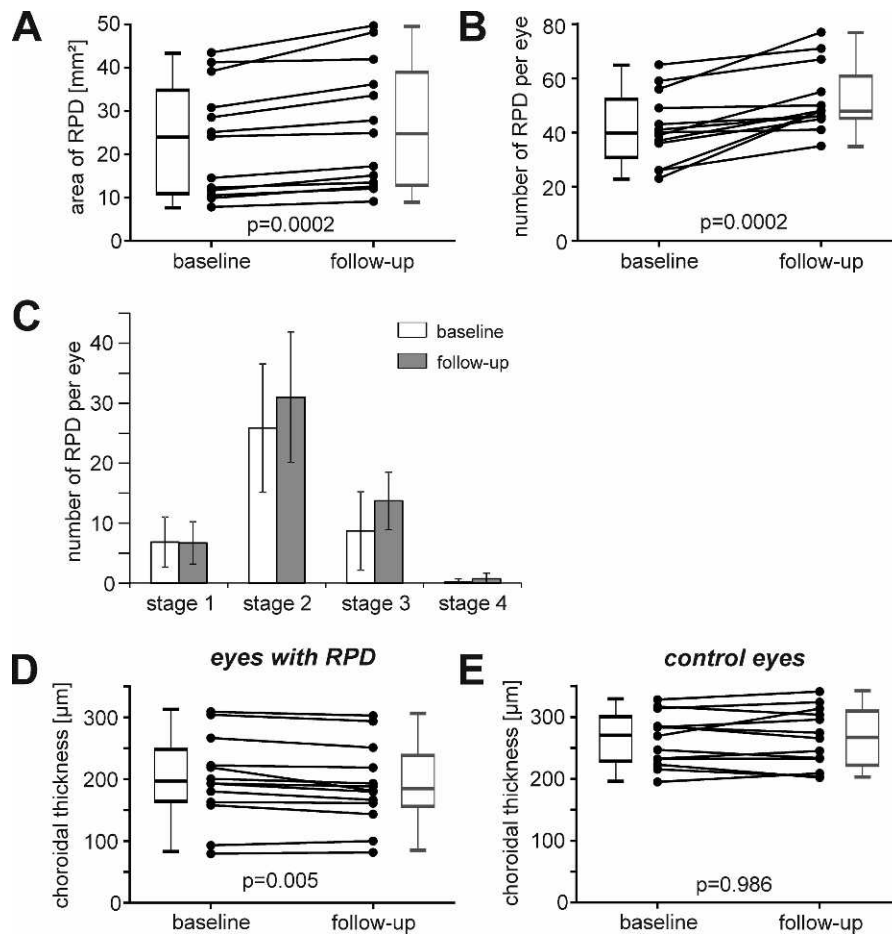


**FIGURE 4.** (A-E) Measurement results of reticular pseudodrusen (RPD) progression parameters at baseline and 12-month follow-up. (A) Size of retinal area affected by RPD. (B) Number of detected RPD lesions per eye. (C) Numbers of RPD per eye exhibiting different stages of the RPD phenotype. (D) Choroidal thickness (CT) in study eyes measured 2000  $\mu\text{m}$  superior to the fovea. (E) CT in healthy control eyes measured 2000  $\mu\text{m}$  superior to the fovea.

summary, mfERG amplitudes decreased to the same extent in both groups.

However, we also compared mfERG amplitudes obtained in areas affected by RPD and corresponding nonaffected areas in the same eye for the follow-up time point, as previously reported for the baseline time point.<sup>15</sup> Whereas there was no significant difference between mfERG amplitudes measured in areas affected by RPD and control areas at baseline, amplitudes differed significantly at the follow-up time point ( $P = 0.001$  for method 1 and  $P = 0.002$  for method 2) (Fig. 6). Changes of amplitudes were found to be significantly different when method 1 was applied ( $P = 0.022$ ), whereas changes differed not significantly with method 2 ( $P = 0.127$ ).

We then compared changes of mfERG amplitudes with changes of the three individual morphologic parameters. No correlations between changes of these parameters and mfERG amplitude changes were found (Fig. 7).

## DISCUSSION

Visual acuity testing reveals foveal function but does not provide a functional map of the central retina. As RPD lesions are predominantly seen perifoveally and foveal architecture itself is usually normal in patients with exclusively RPD, BCVA represents a poor surrogate for a structure/function analysis in RPD patients. Multifunctional ERG is a well-established tech-

nique for functional analysis of the central retina, and previous studies reported a robust intrasession and intersession reproducibility of mfERG measurements.<sup>27,28</sup> The aim of our study was to find correlations between morphologic parameters of RPD progression over time seen in SD-OCT and cSLO imaging and longitudinal changes in retinal function based on mfERG.

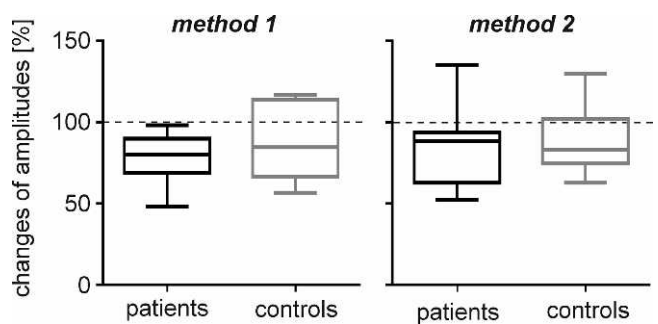


**FIGURE 5.** Comparison of multifocal electroretinography (mfERG) measurements between study eyes and control eyes. The figure shows changes of mfERG amplitudes (%) between baseline and follow-up measurements. Average amplitudes were determined by method 1 and method 2 for each patient and compared to controls. In most cases, amplitudes were smaller at follow-up, and the extent of decrease was almost the same in all groups.

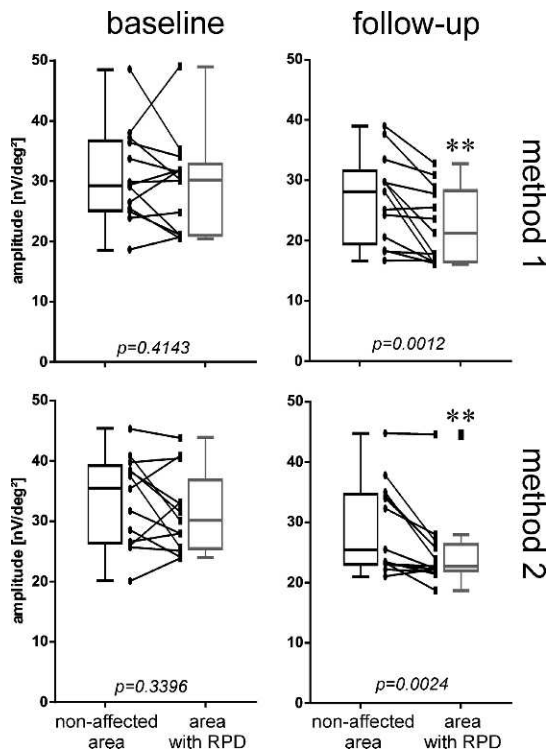


FIGURE 6. Comparison of multifocal electroretinography measurements between RPD-affected and non-RPD-affected areas within the same study eye. Amplitudes were determined by method 1 and method 2 for each study eye at baseline and at follow-up.

Querques and coworkers<sup>16</sup> analyzed RPD progression in SD-OCT over 24 months. They selected only lesions that were judged to show progression over 2 years and found that 100% of RPD lesions graded as stage 1 progressed to stage 2; 81.3% graded as stage 2 at baseline examination progressed to stage 3, and 18.7% progressed to stage 4. All RPD graded as stage 3 at baseline examination progressed to stage 4.<sup>16</sup> In our study, we looked not only at progressive RPD lesions but at the absolute number of RPD lesions to determine changes in the “RPD load” over 1 year. In accordance with Querques et al.,<sup>16</sup> we observed an increase in lesion stages over time and additionally an increase in the number of lesions itself. Notably, RPD progression in terms of height seen in SD-OCT has to be interpreted cautiously. Firstly, the exact placement of follow-up SD-OCT scans compared to baseline, as well as accurate spatial correlation of SD-OCT findings to cSLO images, still remains a crucial challenge for longitudinal analysis of RPD evolution. Secondly, the natural course of RPD development is still poorly understood. Reticular pseudodrusen evolution patterns seem to be quite heterogeneous. Progression and regression of RPD lesions over time have recently been confirmed by Auge and coworkers.<sup>29</sup> The authors emphasize the importance of exact registration of SD-OCT B-scans at different time points as well as the use of very dense volume scans in order to be capable of reliably assessing such discrete intraretinal changes over time.<sup>29</sup> Recently, Spaide<sup>20</sup> reported complete regression of RPD lesions associated with significant changes in the outer retina over 3 years in nearly half of the retrospectively observed patients. The author introduced the term “outer retinal atrophy” describing a degeneration of photoreceptors in the context of RPD regression and considered this phenomenon a new distinct form of late-stage AMD.<sup>20</sup> Consequently, one cannot readily assume that an increase or

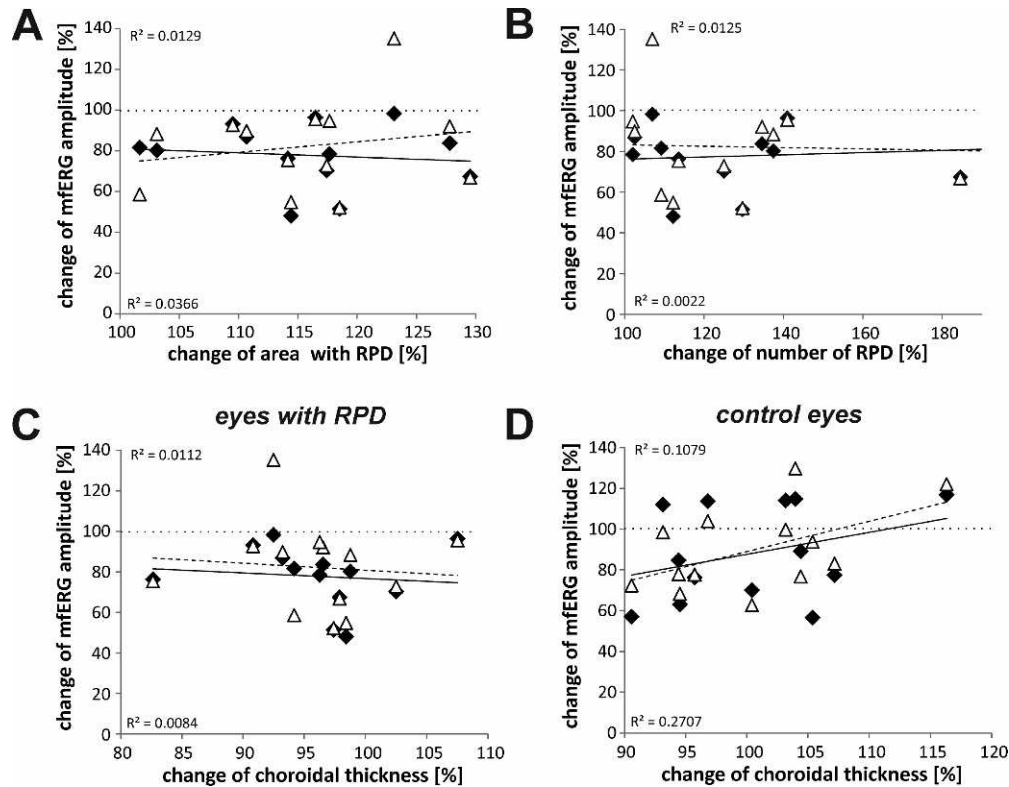


FIGURE 7. (A–D) Correlation of changes of multifocal electroretinography (mfERG) amplitudes with changes of morphological data as follows: (A) area affected by reticular pseudodrusen (RPD), (B) number of RPD, (C) choroidal thickness (CT) in eyes with RPD, (D) CT in control eyes. Values of mfERG amplitudes were determined by method 1 (black diamond, solid line) and method 2 (open triangle, broken line), and no linear correlation was found for the parameters. Correlation coefficients are given in the diagrams (upper left for method 1 and bottom left for method 2). There were also no nonlinear correlations (not shown).

a decrease in RPD lesion stages detected in SD-OCT follow-up scans directly correlates with a disease progression. Based on the current limited knowledge on RPD evolution, we therefore rather interpreted the changes themselves in RPD numbers and RPD stages as a marker for disease activity.

Previous studies reported a reduced CT and choroidal volume in eyes with RPD lesions.<sup>18,19,30</sup> Spaide<sup>20</sup> investigated for the first time the long-term clinical course of eyes with RPD and evaluated, among other parameters, the CT at baseline and at follow-up visits in eyes showing complete regression of RPD lesions. Over a mean 2.9-year follow-up period, the underlying choroid decreased to 81.4% of its initial value. According to the author, eyes with regression of RPD develop outer retinal atrophy and loss of the underlying CT.<sup>20</sup> The study period in our analysis was shorter, and none of our patients showed a complete regression of RPD after 12 months. Nevertheless, we similarly observe a decrease in CT in our RPD patients over time to 96.1%, which, however, turns out to be less considerable than in Spaide's data. Presumably, the unequal study periods sufficiently explain this difference. A general limitation in measuring CT is both the intra- and interindividual variation of the choroidal architecture influenced by numerous factors. Age and refraction represent the most important interindividual factors.<sup>21,22</sup> Both parameters were comparable in the two groups, which significantly reduces CT variation in our analysis. In the future, a more precise delineation of the different layers of the choroid is needed to reveal further insights in pathologic choroidal changes associated with RPD.

Based on three-field composite cSLO FAF imaging, Steinberg et al.<sup>17</sup> observed a continuous enlargement of RPD-affected retinal areas in patients with GA due to AMD, indicating disease progression over time. They reported a mean difference of interobserver agreement of 0.9 mm<sup>2</sup> and a mean growth rate of the RPD-affected area of 4.4 mm<sup>2</sup>/year. Our data show equally reproducible measurements, proving the quality of the previously established measurement technique. Results of the two studies are not entirely comparable, as we did not use composite images for area quantification. In our study, no patient showed RPD-affected retinal areas at the nasal, temporal, or inferior edge of the 30° cSLO image frame. However, in three patients the RPD-affected area exceeded the image frame superiorly. Therefore, the convex hull had to be drawn at the border of the image, and the measured area must be regarded as the minimum RPD extent in these patients. Based on the comparably smaller RPD area growth rate in patients with exclusively RPD compared to GA patients, one may suppose that the presence of GA indicates a higher RPD disease activity. However, the small sample size in our study does not allow definitive conclusions in this regard. Interestingly, Marsiglia and colleagues<sup>31</sup> recently reported that GA expanded particularly into areas previously affected by RPD. Based on these results, the authors postulated that RPD represent an early manifestation of the process leading to GA.<sup>31</sup> In the same year, a study on RPD and multilobular GA by Xu et al.<sup>32</sup> confirmed that GA lobules frequently develop in areas of RPD, strengthening the theory of the same underlying disease process in both phenotypes.

The area quantification method employed in this study does include only the absolute retinal area size of RPD involvement, disregarding the actual number or density of RPD lesions. Measuring two-dimensional progression of RPD extent based on the absolute number of single lesions does not seem reasonable, as single RPD lesions vary considerably in size and often tend to coalesce over time.

Gerth and colleagues<sup>13</sup> reported a progressive loss in mfERG responses in patients with soft drusen over a period of 31 months.<sup>13</sup> Feigl et al.<sup>14</sup> followed retinal function in patients with soft drusen by means of mfERG over 1 year. They

found a significant impairment of retinal function at baseline compared to healthy controls, yet in contrast to Gerth et al.<sup>13</sup> observed no further deterioration after 1 year. The functional results in soft drusen reported in those two studies are not consistent with our findings in patients with exclusively RPD, which may reflect the different impact on photoreceptor integrity of both AMD phenotypes.<sup>14</sup> Mrejen and coworkers<sup>33</sup> investigated the cone photoreceptor mosaic in eyes with RPD using adaptive optics and compared the cone density to that in eyes with soft drusen. Interestingly, they report a dramatic reduction in cone density over RPD lesions possibly due to a change in their orientation, an alteration of their cellular architecture, or even absence of the cones themselves.<sup>33</sup> Based on our mfERG data, a complete absence of cones above RPD lesions seems unlikely. Functional RPD studies with a longer follow-up period than in this study, and particularly functional data on regressing RPD and consequent outer retinal atrophy, are of particular interest and may give further insight in RPD pathophysiology.<sup>20</sup>

A previous report of our group suggested that RPD do not distinctly impact the retinal function seen in mfERG, supporting the theory by Curcio et al.<sup>4</sup> hypothesizing that RPD originate from rod physiology, and therefore, negative impact on rod function was not detected in mfERG.<sup>4,15</sup> However, even if this assumption proves to be correct, it appears unlikely that RPD lesions interfere only with rods and not with cones lying in immediate proximity. In fact, mfERG amplitudes measured in areas affected by RPD and control areas differed significantly at the follow-up time point, demonstrating an effect of progressing RPD on cone function. Nevertheless, this effect appears to be rather small within the observation period, as we could see it only when performing comparison within the affected eyes and not when comparing with healthy controls, which may be due to the small sample size and the statistical spread.

In another structure/function analysis based on microperimetry, Querques and colleagues<sup>34</sup> reported a greater extent of reduced sensitivity in eyes with RPD compared to eyes with typical soft drusen. Similarly, Ooto and coworkers<sup>35</sup> found that distribution and number of RPD lesions are closely associated with retinal sensitivity in microperimetry measurements. Longitudinal data on microperimetry measurements in RPD are not available yet. Although mfERG provides more objective information on retinal function, microperimetry offers a higher spatial resolution and allows for measuring both cone and rod functions.

Obviously, the small number of subjects included in our study and a follow-up period of 12 months preclude any definitive interpretation. Yet patients showing exclusively RPD lesions are rare, and a longer study period increases the risk of developing additional AMD phenotypes like soft drusen, GA, or CNV that would interfere with morphologic and functional measurements.<sup>1</sup> Three patients showed isolated soft drusen at follow-up examination; however, their number in each patient did not exceed three lesions, which makes their impact on morphologic and electrophysiological measurements rather negligible.

With the retinal imaging technology currently available, an exact quantitative and qualitative analysis of RPD progression over time appears challenging, and eventually an estimate remains. The advent of adaptive optics may allow a more reliable stage classification of RPD lesions in the en face image mode as well as an absolute quantitative assessment of the RPD load and its progress over time.<sup>31</sup> Multi-wavelength cSLO imaging also appears promising in characterizing RPD lesion architecture more accurately.<sup>36</sup>

Apparently, the approach of employing a convex polygonal hull for RPD-affected area quantification represents a definite

limitation. Furthermore, retinal area quantification was restricted to the central cSLO image. Presence and evolution of RPD lesions beyond the 30° frames were not documented. Similarly, slight variations in follow-up OCT scan positioning and irregular point-to-point correlation cannot be completely ruled out. The restriction to five high-quality OCT scans limits this uncertainty; however, it produces a selection bias at the same time.

Studying eyes with exclusively RPD and no other signs of AMD raises the question whether these eyes may be attributed to AMD at all and whether these eyes might represent a disease entity itself. Future longitudinal and genetic studies must resolve this issue. In our study group, 11 out of 12 patients showed distinct AMD phenotypes in the fellow eye, which allows us to draw firm conclusions regarding the functional impact of RPD in AMD patients.

A fundamental question in structure/function analysis is whether morphological changes in the outer retina precede functional alterations or vice versa. Based on mfERG and combined cSLO and SD-OCT, our data suggest that RPD lesions can be detected before progression causes functional loss. In the follow-up, differences in changes in mfERG amplitudes between RPD-affected areas and nonaffected areas were still very small. It cannot be ruled out that mfERG is methodologically limited with regard to detecting the earliest functional deficits caused by RPD, or that there are certain compensatory functional mechanisms in the retina when sufficiently small morphological defects are already present, or both. The main signals in the mfERG are derived from cones. Testing only cone function in this perifoveal phenotype certainly represents a further limitation. Current mfERG technology has its limitations concerning spatial resolution. Consequently, an exact correlation of single RPD lesions to mfERG signals cannot be achieved today.

To our knowledge, this is the first study reporting longitudinal structure/function correlations in eyes with RPD. Multifunctional ERG allows for detecting a decline of function over time in eyes with progressive RPD. Functional decline could not be correlated to changes in individual morphologic parameters. Further functional loss due to RPD than detected in our study group presumably occurs at later disease stages, that is, when RPD regression occurs or outer retinal atrophy develops.

### Acknowledgments

The authors thank Verena Lüers for her technical assistance.

Disclosure: **F. Alten**, Novartis (C); **P. Heiduschka**, None; **C.R. Clemens**, Novartis (C); **N. Eter**, Heidelberg Engineering (C), Novartis (C), Bayer (C), Sanofi Aventis (C), Allergan (C), Bausch and Lomb (C)

### References

1. Arnold JJ, Sarks SH, Killingsworth MC, Sarks JP. Reticular pseudodrusen. A risk factor in age-related maculopathy. *Retina*. 1995;15:183-191.
2. Zweifel SA, Imamura Y, Spaide TC, Fujiwara T, Spaide RF. Prevalence and significance of subretinal drusenoid deposits (reticular pseudodrusen) in age-related macular degeneration. *Ophthalmology*. 2010;117:1775-1781.
3. Schmitz-Valckenberg S, Alten F, Steinberg JS, et al.; Geographic Atrophy Progression (GAP) Study Group. Reticular drusen associated with geographic atrophy in age-related macular degeneration. *Invest Ophthalmol Vis Sci*. 2011;52:5009-5015.
4. Curcio CA, Messinger JD, Sloan KR, McGwin G, Medeiros NE, Spaide RF. Subretinal drusenoid deposits in non-neovascular age-related macular degeneration: morphology, prevalence, topography, and biogenesis model. *Retina*. 2013;33:265-276.
5. Sarks J, Arnold J, Ho IV, Sarks S, Killingsworth M. Evolution of reticular pseudodrusen. *Br J Ophthalmol*. 2011;95:979-985.
6. Klein R, Meuer SM, Knudtson MD, Iyengar SK, Klein BE. The epidemiology of retinal reticular drusen. *Am J Ophthalmol*. 2008;145:317-326.
7. Ueda-Arakawa N, Ooto S, Nakata I, et al. Prevalence and genomic association of reticular pseudodrusen in age-related macular degeneration. *Am J Ophthalmol*. 2013;155:260-269.
8. Pumariega NM, Smith RT, Sohrab MA, Letien V, Souied EH. A prospective study of reticular macular disease. *Ophthalmology*. 2011;118:1619-1625.
9. Smith RT, Chan JK, Busuico M, Sivagnanavel V, Bird AC, Chong NV. Autofluorescence characteristics of early, atrophic, and high-risk fellow eyes in age-related macular degeneration. *Invest Ophthalmol Vis Sci*. 2006;47:5495-5504.
10. Sutter EE. The fast m-transform: a fast computation of cross-correlations with binary m-sequences. *SIAM J Comput*. 1991;20:686-694.
11. Sutter EE, Tran D. The field topography of ERG components in man, I: the photopic luminance response. *Vision Res*. 1992;32:433-446.
12. Parisi V, Perillo L, Tedeschi M, et al. Macular function in eyes with early age-related macular degeneration with or without contralateral late age-related macular degeneration. *Retina*. 2007;27:879-890.
13. Gerth C, Hauser D, Delahunt PB, Morse LS, Werner JS. Assessment of multifocal electroretinogram abnormalities and their relation to morphologic characteristics in patients with large drusen. *Arch Ophthalmol*. 2003;121:1404-1414.
14. Feigl B, Brown B, Lovie-Kitchin J, Swann P. Monitoring retinal function in early age related maculopathy: visual performance after 1 year. *Eye (Lond)*. 2005;19:1169-1177.
15. Alten F, Heiduschka P, Clemens CR, Eter N. Multifocal electroretinography in eyes with reticular pseudodrusen. *Invest Ophthalmol Vis Sci*. 2012;53:6263-6270.
16. Querques G, Canoui-Poitrine F, Coscas F, et al. Analysis of progression of reticular pseudodrusen by spectral domain-optical coherence tomography. *Invest Ophthalmol Vis Sci*. 2012;53:1264-1270.
17. Steinberg JS, Auge J, Jaffe GJ, Fleckenstein M, Holz FG, Schmitz-Valckenberg S. Longitudinal analysis of reticular drusen associated with geographic atrophy in age-related macular degeneration. *Invest Ophthalmol Vis Sci*. 2013;54:4054-4060.
18. Alten F, Clemens CR, Heiduschka P, Eter N. Localized reticular pseudodrusen and their topographic relation to choroidal watershed zones and changes in choroidal volumes. *Invest Ophthalmol Vis Sci*. 2013;54:3250-3257.
19. Querques G, Querques L, Forte R, Massamba N, Coscas F, Souied EH. Choroidal changes associated with reticular pseudodrusen. *Invest Ophthalmol Vis Sci*. 2012;53:1258-1263.
20. Spaide RF. Outer retinal atrophy after regression of subretinal drusenoid deposits as a newly recognized form of late age-related macular degeneration. *Retina*. 2013;33:1800-1808.
21. Fujiwara T, Imamura Y, Margolis R, Slakter JS, Spaide RF. Enhanced depth imaging optical coherence tomography of the choroid in highly myopic eyes. *Am J Ophthalmol*. 2009;148:445-450.
22. Margolis R, Spaide RF. A pilot study of enhanced depth imaging optical coherence tomography of the choroid in normal eyes. *Am J Ophthalmol*. 2009;147:811-815.
23. Zweifel SA, Spaide RF, Curcio CA, Malek G, Imamura Y. Reticular pseudodrusen are subretinal drusenoid deposits. *Ophthalmology*. 2010;117:303-312.

24. Schmitz-Valckenberg S, Bindewald-Wittich A, Dolar-Szczasny J, et al. Correlation between the area of increased autofluorescence surrounding geographic atrophy and disease progression in patients with AMD. *Invest Ophthalmol Vis Sci.* 2006;47:2648-2654.
25. Hood DC, Bach M, Brigell M, et al. ISCEV standard for clinical multifocal electroretinography (mfERG) (2011 edition). *Doc Ophthalmol.* 2012;124:1-13.
26. Frigge M, Hoaglin DC, Iglewicz B. Some implementations of the boxplot. *Am Stat.* 1989;43:50-54.
27. Meigen T, Friedrich A. The reproducibility of multifocal ERG recordings [in German]. *Ophthalmologe.* 2002;99:713-718.
28. Gundogan FC, Sobaci G, Bayraktar MZ. Intra-session and inter-session variability of multifocal electroretinogram. *Doc Ophthalmol.* 2008;117:175-183.
29. Auge J, Steinberg JS, Fleckenstein M, Holz FG, Schmitz-Valckenberg S. Reticular drusen over time with SD-OCT [in German] [published online ahead of print October 3, 2013]. *Ophthalmologe.*
30. Garg A, Oll M, Yzer S, et al. Reticular pseudodrusen in early age-related macular degeneration is associated with choroidal thinning. *Invest Ophthalmol Vis Sci.* 2013;54:7075-7081.
31. Marsiglia M, Boddu S, Bearely S, et al. Association between geographic atrophy progression and reticular pseudodrusen in eyes with dry age-related macular degeneration. *Invest Ophthalmol Vis Sci.* 2013;54:7362-7369.
32. Xu L, Blonska AM, Pumariega NM, et al. Reticular macular disease is associated with multilobular geographic atrophy in age-related macular degeneration. *Retina.* 2013;33:1850-1862.
33. Mrejen S, Sato T, Curcio CA, Spaide RF. Assessing the cone photoreceptor mosaic in eyes with pseudodrusen and soft drusen in vivo using adaptive optics imaging. *Ophthalmology.* 2014;121:545-551.
34. Querques G, Massamba N, Srour M, et al. Impact of reticular pseudodrusen on macular function. *Retina.* 2014;34:321-329.
35. Ooto S, Ellabban AA, Ueda-Arakawa N, et al. Reduction of retinal sensitivity in eyes with reticular pseudodrusen. *Am J Ophthalmol.* 2013;156:1184-1191.
36. Alten F, Clemens CR, Heiduschka P, Eter N. Characterization of reticular pseudodrusen and their central target aspect in multi-spectral confocal scanning laser ophthalmoscopy. *Graefes Arch Clin Exp Ophthalmol.* 2014;252:715-721.